Analysis of the Influence Of Friction Stir Welding on the Microstructure and Mechanical Properties of Alloy UNS-C27200 (CU-ZN)

Renato F. Rosa[a*] [iD] *, Italo O. Almeida*[a]*, Francisco M. F. A. Varasquim*[a,b] [iD] *, Eli J. C. Junior*[b]*,*

Antônio A. Couto[c]*, Vinicius T. Santos*[d]*, Márcio R. Silva*[d]*, Francisco Y. Nakamoto*[a]*, Givanildo A. Santos*[a]

[a]*Instituto Federal de Educação, Ciência e Tecnologia de São Paulo, Programa de Pós-Graduação em Engenharia Mecânica, Campus São Paulo, São Paulo, SP, Brasil.*
[b]*Instituto Federal de Educação, Ciência e Tecnologia de São Paulo, Departamento de Engenharia Mecânica, Campus Itapetininga, São Paulo, SP, Brasil.*
[c]*Universidade Presbiteriana Mackenzie, São Paulo, SP, Brasil.*
[d]*Termomecanica São Paulo S/A, Centro de Pesquisa e Desenvolvimento de Ensaios, São Bernardo do Campo, SP, Brasil.*

The copper alloy UNS-C27200 is a binary brass, composed of 38wt%Zn, beeing one of the most used in the industry. The union of Cu-Zn alloys by conventional welding by fusion in thin plates presents several challenges. The Friction Stir Welding (FSW) process performs the union of two, or more materials, through a rotating tool that travels throughout the welding region. One the great advantages of FSW is working below the melting point of the material, which reduces the change in the microstructure and properties of the material, when compared to conventional welding processes. Due to the lack of research on FSW process in lap brass joints with thin thicknesses, the present work aims to expand these studies in order to contribute to future research. Eight conditions were evaluated, varying rotation and welding speed. In the best results by visual inspection, analyzes of microstructure, temperature, microhardness and mechanical strength were performed. The better welding results were obtained with ω=1050 rpm and v=20 mm/min. There was reduction of approximately 50% between Stir Zone and Base metal. The mechanical strength was affected by the pin hole resulting from the process. The microstructure revealed a homogeneous mixture in the stir zone and no defects were detected.

Keywords: *Friction stir welding - FSW, lap joint, UNS-C27200, mechanical behavior.*

1. Introduction

The Cu without alloy element is very soft, ductile, easy to work cold, but has low mechanical strength. It has great application when require high corrosion resistance and high electrical conductivity. To improve some of its characteristics, cold working processes and/or alloy formation by solid solution are often used, where small amounts of alloying elements are often added[1,2].

The most common and used copper alloys in the industry are binary brasses (Cu-Zn), zinc (Zn) being the main alloy element[1,2]. The copper alloy UNS-C27200 is a binary brass, composed of 38%Zn. For being a brass α+ß, exhibits better weldability[2] than the brasses-α and is more malleable than copper and zinc[2]. It has a relatively low melting point ranging from 800 to 1070°C, depending on the zinc value in its composition, and in general the higher the amount of zinc, the lower the melting point[3].

In addition to the above-mentioned characteristics, the UNS-C27200 alloy offers very useful properties such as high strength, good conductivity, conformability, wear resistance and corrosion performance, deep stamping and intense gloss of strong golden color[3,4].

The union of Cu-Zn alloys by conventional welding by fusion in thin plates presents several challenges[4], because the temperatures obtained in these processes are high and cause partial evaporation of zinc[5] due to its low boiling point (907°C), bringing several problems in the weld region, such as surface irregularities, major distortions, cracks, color change due to oxidation, porosity and others arising from solidification[6,7].

In order to minimize these problems, in 1991 TWI (The Welding Institute) developed a welding technique called Friction Stir Welding – FSW, which is a welding process that occurs in the solid state, where it is possible to join parts with working temperature below the melting temperature[8]. Figure 1 show the principal variables in FSW process.

Initially this technique was developed for welding Al alloys, but its great potential led several researchers[4,10-14] to apply this technique in the welding of Mg, Cu, Ti, Al, lead, some steels, thermoplastics and different combinations of materials, particularly those with nearby melting temperatures and similar behavior, such as hot workability.

The FSW process in lap joints is not complex[5,9,15-17]. A non-consumable rotating tool - formed by pin and shoulder - is dipped between the plates mixing the material and then the tool is displaced, forming the weld profile[18].

*e-mail: renatofrosa3@gmail.com

The kinetic energy of the tool is transformed into thermal energy, generated by friction at the interface between the pin and the shoulder of the tool and the parts to be welded, causing the material to reach high temperature and is in a plasticized state[19]. As the tool moves, the plasticized material is stirred and forged by the shoulder face, where it consolidates and cools to form a solid phase bond between the two pieces[10]. Due to the intense plastic deformation that happens in the stir, the weld formation mechanism is described by some researchers[10,15,20] as a combination of extrusion and forging, where the working temperature is less than the melting point of the materials to be joined together.

The FSW process involves several variables[10,21,22], which together contribute to obtain a quality welded joint, with rotation speed (ω) and welding speed (v) being the most prominent parameters[23].

Although there are several important results in the studies of FSW in butt joints[3,12,22-24], greater efforts are needed in research for FSW in lap brass joints with thin thicknesses, both with similar materials and in dissimilar materials, given the few publications found with this welding configuration[5,15,16,24].
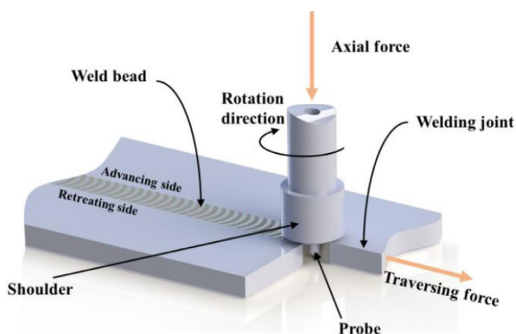

Figure 1. Typical welding procedure by a rotating shoulder[9].

2. Materials and Methods

The welds were processed using rectangular, rolled and annealed plates of UNS-C27200 brass, hardness grade ½ hard, with 2 mm thicknesses. Tables 1 and 2 show the chemical compositions and mechanical properties of the material.

All samples were joined in the configuration of lap joints according to Figure 2a, with weld length of 50 mm. The samples dimensions were 100x20x2, length, width and thickness, respectively. A rotating tool with shoulder and tapered pin, in H13 tool steel, quenched e tempered with 50~55 HRC according to Figure 2b was used. A device is designed to provide the necessary process stiffness, plate fixing, and tool tilt angle relative to the Z axis (3°).

For temperature monitoring, a system with Arduino programming and CoolTerm freeware software was developed, 4 k-type thermocouples (T1, T2, T3 and T4) were used, with stainless steel tip and M6 x 12 thread. The thermocouples were mounted on the device to obtain the temperature at the bottom of the plates as shown in Figure 3. Although the measured values did not correspond to the actual temperatures, they served as the basis for observing the temperature distribution during the FSW process.

The welds were performed in a 3-axis Veker Machining Center, model MV-760-ECO, with computerized numerical control (CNC). The process parameters were based on literature data published by[2,5,7,16,18,22] and refined by preliminary tests to provide the best parameter capable of producing welding visually without defects.

Preliminary tests were produced according to the data shown in Table 3, maintaining constant the other parameters such as dwelt time = 5s, penetration speed = 10 mm/min, shoulder penetration = 0.2 mm and pin lentht = 3.7 mm. For each combination in Table 3, 4 replicates were performed, totaling 32 experiments.
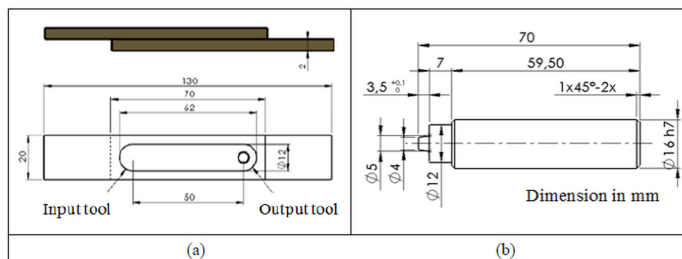

Figure 2. (a) Lap joint welding configuration; (b) Welding tool design.

Table 1. Chemical composition (wt%) of brass plates UNS-C27200 (Cu38Zn).

Cu	Zn	Fe	Pb	P	Sn
61.90	37.98	0.02	0.01	0.01	0.01

Table 2. Mechanical properties of the brass plates UNS-C27200 (Cu38Zn).

Alloy	Ultimate tensile strength [MPa] min.	Yield strength 0.2% [MPa]	Elongation [%] min.	Modulus of elasticity [MPa]
UNS-C27200	370	250	27	103000

The microhardness tests were performed in a Buehler microdurometer on the Vickers HV scale with a load of 0.1kgf, using as reference the ASTM E384 standard[25].

The selected samples were sectioned in the plane perpendicular to the welding direction, embedded in bakelite and were submitted to a sanding and polishing process according to standard procedures. They were chemically attacked by immersion of the samples in an ethyl alcohol-based reagent composed of 10.7% hydrochloric acid and 3.4% of ferric chloride for 25 seconds.

The weld strength was evaluated by shear tests in a universal test machine EMIC DL 10000, TRD 28 cell, traction load 100 kN with test speed of 5 mm/min.

3. Results and Discussion

3.1. Visual inspection

The welded joints were evaluated by visual inspection with the naked eye, without the aid of any instrument. Figure 4 reproduces the surface of welded joints with the combinations defined in Table 3.

Not all parameters surveyed generated welds without apparent defects for UNS - C27200 brass samples. Figure 4 shows the tunnel defects in the stirred zone, which is commonly caused by insufficient heat[10]. It was observed on the advanced side and was linearly located along the weld line under welding conditions ω = 750, 850 and 950 rpm. The tunnel defect appeared in all samples welded with v = 60 mm/min, being smaller with v = 20 mm/min.

Table 3. Combinations used for sample production.

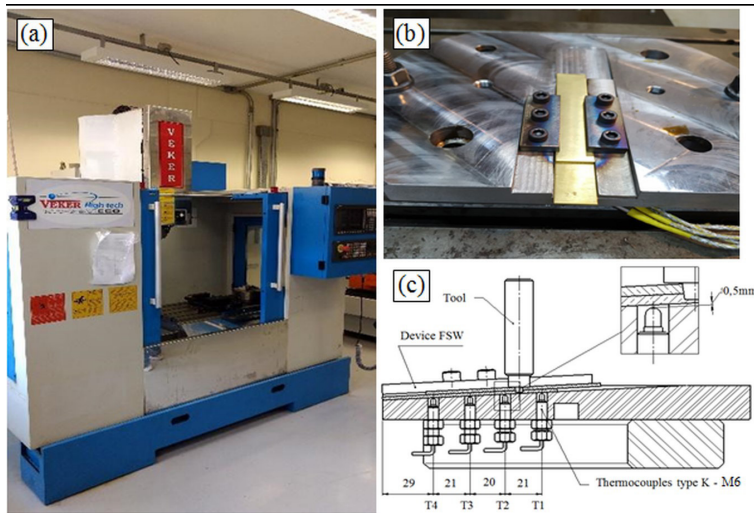| Combination of Experiments (C)	ω [rpm]	v [mm/min]
C1	750	20
C2		60
C3	850	20
C4		60
C5	950	20
C6		60
C7	1050	20
C8		60

Figure 3. (a) Adaptaded machine used in process, (b) welding device and (c) position of thermocouples type-k in welding device (dimensions in mm).
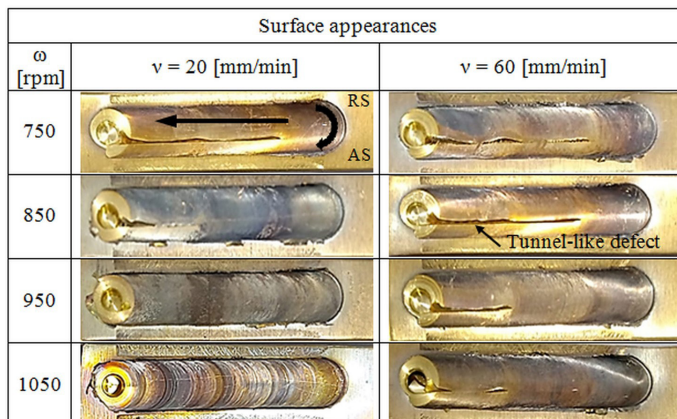

Figure 4. Surface appearances of the welds.

From the visual inspections, the combination that showed the best results, such as filling the weld bead, no tunnels on the weld surface and minimal flash, were those obtained with ω = 1050 rpm and v = 20 mm/min (combination C7). The other procedures and results will be based on the welds produced with these parameters.

3.2. Temperature

In order to better understand the mechanisms involved in the formation of microstructures and the behavior of zinc in alloy, temperature values were measured at the bottom of the plates[16]. Due to the characteristics of the FSW process, we can observe that the working temperature was below the melting temperature of the alloy under study (920°C) and the boiling temperature of zinc (907°C), as shown in Figure 5. The temperatures obtained are satisfactory, as it avoided the reduction of the percentage of zinc by evaporation and consequently the formation of pores in the welded region[3].
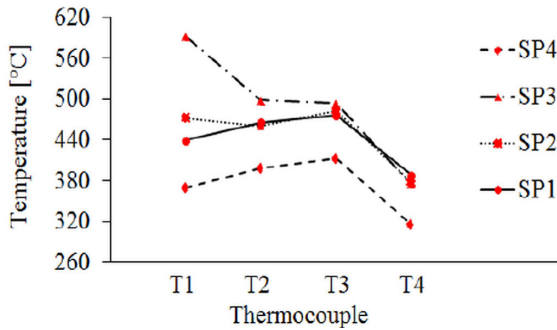
3.3. Microhardness

Figure 6a shows the position where the microhardness was measured, where "BP" is the line between plates, "L1" and "L2" the lines of the upper plate and "L3" and "L4" the lines of the lower plate. Vertical distances are 0.5 mm. Figure 6b shows the hardness profiles found in the specimen.

The specimen showed a reduction in hardness in the stirred zone when compared to the base metal. Although large differences in hardness are observed on the advancing side, where there is a high concentration of heat due to the drag of material to the retreating side[26], the stirred zone presents a considerable difference as observed in Figure 6b. The temperature peak is obtained precisely in the symmetry line of the joint, being a region of visual identification facilitated, with greater guarantee for the analysis[27]. There is also the contribution of the pin shape, because the tapered pin results in temperatures higher than the cylindrical pin[19] and the axial force is also higher, so that this increased heat generation in the hot condition, causing a significant reduction in the average hardness to 80.4 HV0.1 when compared to the base metal of 179 HV0.1.

3.4. Shear tensile tests

The strength of the joint was evaluated by shear tensile test, following the procedure adopted by[15,16] and ASTM Standard E8/E8M[28], which the specimens and their dimensions are shown in Figure 2a. For this test four specimens were tested. The results of maximum stress obtained and two images, one from the top and other from base, of each specimen is shown in Figure 7.

The weld region remained intact in all specimens and the rupture of the base metal occurred on the output side of the tool, where the hole left by the pin caused a reduction of the resistant area, favoring the rupture.
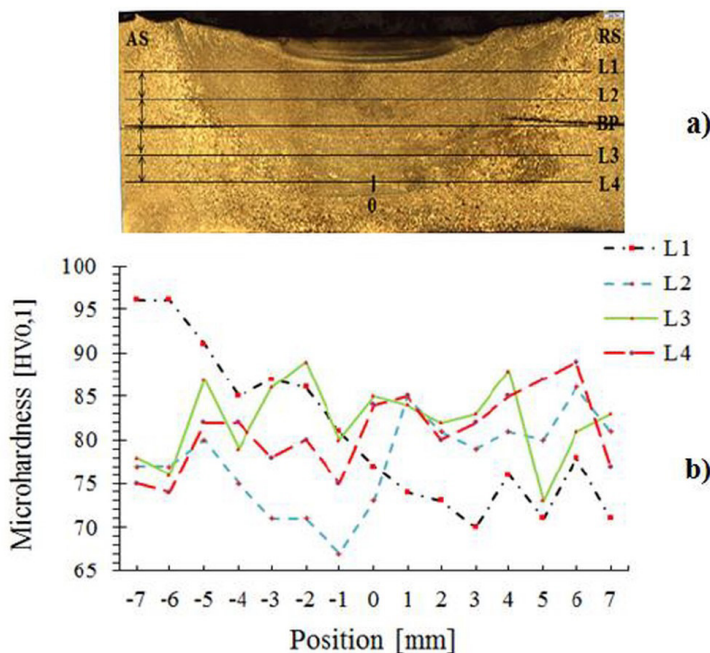
Figure 5. Temperatures obtained in specimens (SP).

Figure 6. (a) Position of the lines for measuring microhardness; (b) Microhardness profiles in cross section with ω = 1050 rpm and v = 20 mm/min.

The joints showed some dispersion in the shear test, indicating a less stable result. It is possible that the temperature increase, that is, a higher heat intake influenced the contact condition, causing the tool to slip[21]. An 48% joint efficiency of Cu was reached in relation to base metal. Temperture doesn't affect the results on tensiles properties.

3.5. Microstructure

The typical macrograph of the cross-section of the lap welded UNS-C27200 alloy is shown in Figure 8. The macrostructure has a very similar appearance to studies of[18,23] where the shape of the stirred zone resembles a wine cup; this format may vary according to welding parameters, tool type and material characteristics.

Microstructural evolution in the perpendicular plane can be seen in Figure 9, where three different zones can be clearly identified, i.e., the stirred zone (SZ), the thermo-mechanically affected zone (TMAZ) and the base metal (BM)[23].

The following microstructures show the structural changes obtained in the FSW process. In Figure 10a the SZ presents equiaxial and refined grains, resulting from the intense stir of materials and complete dynamic recrystallization[22,23]. In Figure 10b TMAZ, which due to severe plastic deformation and intense heat generation is the target of microstructural changes that, in turn, cause significant changes in mechanical properties. This region is not completely recrystallized and has structural changes from the region that encompasses the shoulder width to the pin near the root[20].

Figure 10c and d shows the SZ surrounded by TMAZ with significantly different microstructure. It is possible to observe the progressive increase in the grain size of the TMAZ when moving away from the SZ[3]. The transition between SZ and TMAZ was more evident on retreating side than the advanced side.

Specimens	Maximum stress [MPa]	Top side from plates	Base side from plates
1	291.714		
2	279.803		
3	369.428		
4	304.434		

Figure 7. Maximum stress obtained and images from the tested specimens.

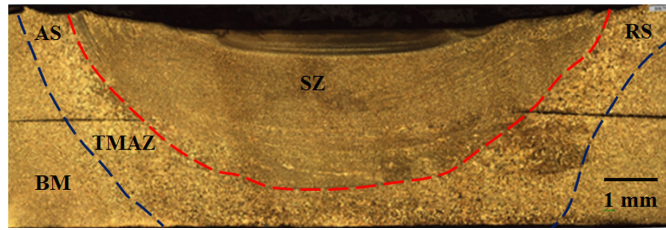**Figure 8.** Cross section of lap joint processed with ω = 1050 rpm and v = 20 mm/min.

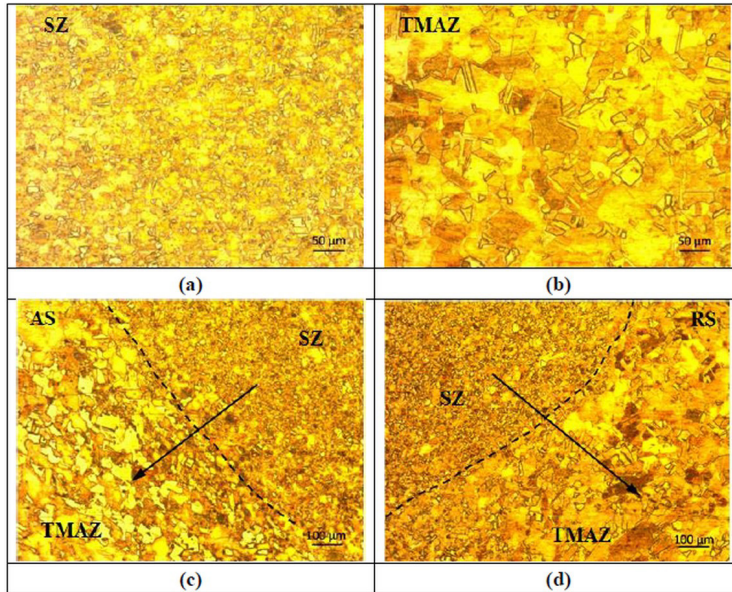**Figure 9.** Macrostructure of the welded joint and its zones.

Figura 10. Microstructures obtained in the FSW process.

4. Conclusions

In this study, the microstructural evolution and mechanical properties of an UNS-C27200 brass alloy were investigated. Based on the results, the main conclusions are as follows:

- The process parameters with ω = 1050 rpm and v = 20 mm/min produced welds without defects such as cavities, voids and tunnels on the weld surface.
- All the specimens approved in the visual inspection ruptured in the pin hole left and there was no separation of the plates.
- There was a significant hardness reduction of 40 to 50% between SZ and BM in the weld setting with ω = 1050 rpm and v = 20 mm/min.
- After analysis of macrostructure and microstructure, it was found that there was a homogeneous mixture in the SZ.

5. Acknowledgements

6. References

1. Callister WD, Rethwisch DG. Materials science and engineering: an introduction. Hoboken: Nj Wiley; 2016.
2. Çam G, Serindağ HT, Çakan A, Mistikoglu S, Yavuz H. The effect of weld parameters on friction stir welding of brass plates. Materialwiss Werkstofftech. 2008;39(6):394-9.
3. Emamikhah A, Abbasi A, Atefat A, Givi MKB. Effect of tool pin profile on friction stir butt welding of high-zinc brass (CuZn40). Int J Adv Manuf Technol. 2013;71(1-4):81-90.
4. Çam G. Friction stir welded structural materials: beyond Al-alloys. Int Mater Rev. 2011;56(1):1-48.
5. Gharavi F, Ebrahimzadeh I, Amini K, Darya P. Evaluation of the microstructure and mechanical properties of friction stir-welded copper/brass dissimilar joints. Mater Res Express. 2018;5(7):076517.
6. Heidarzadeh A, Saeid T, Klemm V. Microstructure, texture, and mechanical properties of friction stir welded commercial brass alloy. Mater Charact. 2016;119:84-91.
7. Meran C. The joint properties of brass plates by friction stir welding. Mater Des. 2006;27(9):719-26.
8. The Welding Institute: TWI. Materials joining technology [Internet]. Cambridge: TWI Ltd; 2020 [cited 2020 Mar 20]. Available from: www.twi.co.uk
9. Eslami S, Ramos T, Tavares PJ, Moreira PMGP. Effect of friction stir welding parameters with newly developed tool for lap joint of dissimilar polymers. Procedia Eng. 2015;(114):199-207.
10. Mishra RS, Ma ZY. Friction stir welding and processing. Mater Sci Eng Rep. 2005;50(1-2):1-78.

11. Lee WB, Lee CY, Chang WS, Yeon YM, Jung SB. Microstructural investigation of friction stir welded pure titanium. Mater Lett. 2005;59:3315-8.

12. Dias LV, Vaz CT. União de termoplásticos pelo processo friction stir welding: influência da ferramenta e parâmetros do processo. Soldag Insp. 2021;26:e2541.

13. Serindag HT, Kiral BG. Friction stir welding of AZ31 magnesium alloys - a numerical and experimental study. Lat Am J Solids Struct. 2017;14(1):113-30.

14. Tarkono T, Tenando F, Nafrizal N, Sukmana I. The effect of rotational speed on Friction Stir Welding (FSW) Quality of dissimilar aluminum alloy series AA 1100 and AA 5052. Jurnal Polimesin. 2023;21(1):21-4.

15. Abdollah-Zadeh A, Saeid T, Sazgari B. Microstructural and mechanical properties of friction stir welded aluminum/copper lap joints. J Alloys Compd. 2008;460(1-2):535-8.

16. Wiedenhöft AG, de Amorim HJ, Rosendo T S, Tier MAD, Reguly A. Effect of heat input on the mechanical behaviour of Al-Cu FSW lap joints. Mater Res. 2018;21(4):e20170983.

17. Ghiasvand A, Ranjbarnodeh E, Mirsalehi SE. The microstructure and mechanical properties of single-pass and double-pass lap joint of Al 5754H-11 and Mg AZ31-O alloys by friction stir welding. J Mater Res Technol. 2023;23:6023-38.

18. Park HS, Kimura T, Murakami T, Nagano Y, Nakata K, Ushio M. Microstructures and mechanical properties of friction stir welds of 60% Cu–40% Zn copper alloy. Mater Sci Eng A. 2004;371(1-2):160-9.

19. Buffa G, Hua J, Shivpuri R, Fratini L. Design of the friction stir welding tool using the continuum based FEM model. Mater Sci Eng A. 2006;1-2(419):381-8.

20. Thomas WM, Threadgill PL, Nicholas ED. Feasibility of friction stir welding steel. Sci Technol Weld Join. 1999;4(6):365-72.

21. Ericsson M, Sandström R. Influence of welding speed on the fatigue of friction stir welds, and comparison with MIG and TIG. Int J Fatigue. 2003;25(12):1379-87.

22. Srinivas P, Ali A. Effect of friction stir welding (FSW) on mechanical properties and microstructure of naval brass C46400. J Xidian Univ. 2020;14(5):3921-3947.

23. Moghaddam MS, Parvizi R, Haddad-Sabzevar M, Davoodi A. Microstructural and mechanical properties of friction stir welded Cu–30Zn brass alloy at various feed speeds: influence of stir bands. Mater Des. 2011;32(5):2749-55.

24. Sun Y, Gong W, Feng J, Lu G, Zhu R, Li Y. A review of the friction stir welding of dissimilar materials between aluminum alloys and copper. Metals. 2022;12(4):675.

25. ASTM: American Society for Testing and Materials. ASTM E384: standard test method for microindentation hardness of materials. 17th ed. West Conshohocken: ASTM International; 2017. 40 p.

26. Vilaça P, Quintino L, dos Santos JF. iSTIR: analytical thermal model for friction stir welding. J Mater Process Technol. 2005;3(169):452-65.

27. Boz M, Kurt A. The influence of stirrer geometry on bonding and mechanical properties in friction stir welding process. Mater Des. 2004;4(25):343-7.

28. ASTM: American Society for Testing and Materials. ASTM E8/E8M: standard test methods for tension testing of metallic materials. 16th ed. West Conshohocken: ASTM International; 2016. 30 p.